frontiers | Frontiers in Immunology

TYPE Original Research
PUBLISHED 23 December 2024
DOI 10.3389/fimmu.2024.1500570

OPEN ACCESS

EDITED BY
Jingying Zhou,
The Chinese University of Hong Kong, China

REVIEWED BY
Nicolas Boisgerault,
INSERM U1307 - CRCI2NA, France
Hailiang Wang,
Qingdao University, China

*CORRESPONDENCE
Victoria A. Jennings
vicki.jennings@york.ac.uk

†PRESENT ADDRESS
Victoria A. Jennings,
Jack Birch Unit for Molecular Carcinogenesis, Department of Biology & York Biomedical Research Institute, University of York, York, United Kingdom

‡These authors share last authorship

RECEIVED 23 September 2024
ACCEPTED 29 November 2024
PUBLISHED 23 December 2024

CITATION
Jennings VA, Rumbold-Hall R, Migneco G, Barr T, Reilly K, Ingram N, St Hilare I, Heaton S, Alzamel N, Jackson D, Ralph C, Banerjee S, McNeish I, Bell JC, Melcher AA, Ilkow C, Cook GP and Errington-Mais F (2024) Enhancing oncolytic virotherapy by extracellular vesicle mediated microRNA reprograming of the tumour microenvironment. *Front. Immunol.* 15:1500570. doi: 10.3389/fimmu.2024.1500570

Enhancing oncolytic virotherapy by extracellular vesicle mediated microRNA reprograming of the tumour microenvironment

Victoria A. Jennings[1*†], Reah Rumbold-Hall[1], Gemma Migneco[1], Tyler Barr[1], Katrina Reilly[1], Nicola Ingram[1], Isabelle St Hilare[2], Samuel Heaton[1], Noura Alzamel[1], David Jackson[3], Christy Ralph[3], Susan Banerjee[4], Iain McNeish[5], John C. Bell[2], Alan A. Melcher[6], Carolina Ilkow[2], Graham P. Cook[1‡] and Fiona Errington-Mais[1‡]

[1]Leeds Institute of Medical Research, School of Medicine, University of Leeds, St. James University Hospital, Leeds, United Kingdom, [2]Center for Innovative Cancer Therapeutics, Ottawa Hospital Research Institute, Ottawa, ON, Canada, [3]Leeds Cancer Centre, St James's Hospital, Leeds, United Kingdom, [4]The Royal Marsden Hospital, Fulham Road, London, United Kingdom, [5]Department of Cancer and Surgery, Imperial College London, London, United Kingdom, [6]The Institute of Cancer Research, Divisions of Radiotherapy and Imaging and Breast Cancer Research, Chester Beatty Laboratories, London, United Kingdom

Background: There has been limited success of cancer immunotherapies in the treatment of ovarian cancer (OvCa) to date, largely due to the immunosuppressive tumour microenvironment (TME). Tumour-associated macrophages (TAMs) are a major component of both the primary tumour and malignant ascites, promoting tumour growth, angiogenesis, metastasis, chemotherapy resistance and immunosuppression. Differential microRNA (miRNA) profiles have been implicated in the plasticity of TAMs. Therefore, delivering miRNA to TAMs to promote an anti-tumour phenotype is a novel approach to reverse their pro-tumour activity and enhance the efficacy of cancer immunotherapies. Oncolytic viruses (OVs) preferentially replicate in tumour cells making them ideal vehicles to deliver miRNA mimetics to the TME. Importantly, miRNA expressed by OVs get packaged within tumour-derived extracellular vesicles (TDEVs), and release of TDEV is augmented by OV infection, thus enhancing the dissemination of miRNA throughout the TME.

Method: Small RNA sequencing was used to identify differentially expressed miRNA during TAM generation and following LPS/IFNγ stimulation to induce an anti-tumour phenotype. Two differentially expressed miRNA identified, miR-155 and miR-19a, were cloned into oncolytic rhabdovirus (ORV), and anti-tumour efficacy was investigated using both *in vitro* and *in vivo* models of OvCa.

Results: This study demonstrates that ORV infection enhances TDEV production in OvCa cell lines both *in vitro* and *in vivo* and that TDEV are preferentially taken up by myeloid cells, including TAMs. Small RNA sequencing identified 23 miRNAs that were significantly upregulated in anti-tumour TAMs, including miR-155-5p. While 101 miRNAs were downregulated during pro-tumour TAM differentiation, including miR-19a-3p. Culturing TDEV expressing miR-155 or miR-19a with TAMs reversed their immunosuppressive activity, as measured by T cell

proliferation. While ORV-miR-155 enhanced the generation of anti-tumour T cells, only ORV-miR19a significantly improved survival of mice bearing ovarian tumours.

Conclusion: This study demonstrates (i) that arming ORVs with immunomodulatory miRNA is an effective approach to deliver miRNA to myeloid cells within the TME and (ii) that miRNA have the capacity to reverse the tumour promoting properties of TAMs and improve the efficacy of cancer immunotherapies, such as OV.

KEYWORDS

oncolytic virus, miRNA, tumour associated macrophage, tumour microenvironment, anti-tumour immunity

Highlights

- What is already known on this topic: miRNA expression is critical in driving macrophage polarisation by simultaneously regulating expression of multiple cellular targets. Reintroducing miRNA to promote an anti-tumour macrophage phenotype is a promising therapeutic approach to reverse the immunosuppressive function of tumour associated macrophages.
- What this study adds: This study shows that extracellular vesicles from virally infected tumour cells are preferentially taken up by myeloid cells, this cell-to-cell communication can be hijacked by oncolytic rhabdoviruses expressing miRNA to deliver miRNA molecules to myeloid cells directly within the tumour microenvironment, which are not intrinsically permissive to direct infection.
- How this study might affect research, practice or policy: This study demonstrates that encoding immunomodulatory miRNA into oncolytic rhabdoviruses' is an effective approach to modulate the immunosuppressive tumour microenvironment and enhance anti-tumour immunity following oncolytic virotherapy.

Introduction

Each year in the UK, approximately 7500 new cases of ovarian cancer (OvCa) are diagnosed and ~4100 deaths are reported: high-grade serous ovarian cancer (HGSOC) accounts for 75% of these deaths (1). Standard treatments of debulking surgery and platinum-based chemotherapy have limited efficacy in advanced disease, with a 5-year survival rate of only ~25%. Recently, poly-ADP ribose polymerase inhibitors (PARPi) have demonstrated efficacy in patients with deficient homologous recombination (HR). Unfortunately, PARPi are less effective in cancers with proficient HR (~50% of patients); moreover, acquired drug resistance and relapse remains a clinical problem (2). Therefore, new therapeutic approaches are required.

Cancer immunotherapies have revolutionised treatment for several malignancies, including melanoma, offering the potential of long-lasting anti-tumour immunity. Unfortunately, HGSOC does not respond well to current immunotherapy, e.g., immune checkpoint blockade (ICB; ~10-15% response) (3). However, as cancer immunotherapies have the potential to generate long-lasting cancer remissions, developing approaches to enhance their efficacy is essential.

Successful OvCa immunotherapy requires the inhibitory effects of the immunosuppressive tumour microenvironment (TME) to be overcome, tipping the balance in favour of anti-cancer immune responses. The immunosuppressive TME of OvCa is unique among other solid tumours since cancer cells are continuously shed from the primary tumour into the peritoneal cavity, seeding new sites of cancer growth and creating a build-up of fluid known as malignant ascites. Tumour-associated macrophages (TAMs) are a major component of both the primary tumour and malignant ascites, and are a critical component of the OvCa microenvironment, promoting tumour growth, angiogenesis, metastasis, chemoresistance and immunosuppression.

Oncolytic viruses (OVs) are naturally occurring, attenuated or genetically modified viruses which preferentially replicate in and lyse tumour cells, leaving healthy cells unharmed. Oncolytic virotherapy is a novel form of cytotoxic immunotherapy and several OVs have demonstrated the ability to infect and lyse OvCa cells, including primary OvCa cells isolated from patient ascites (4–6). The ability to genetically modify OVs to encode immune-stimulatory factors (such as pro-inflammatory cytokines) has been exploited in several cancers (7–9).

Dysregulation of miRNA profiles has been reported for many cell types in the TME, not only tumour cells, but also cancer-associated fibroblast (CAFs), endothelial cells and immune cells (10–13). The aim of this study was to identify miRNA that are either highly expressed in anti-tumour immune phenotypes or are lost during tumour progression and reintroduce these miRNAs using oncolytic rhabdoviruses (ORV) vectors, with the aim of improving

the generation of anti-tumour immunity following oncolytic virotherapy. Importantly, our previously published work has demonstrated that expressing miRNA from ORV results in virally expressed miRNAs being disseminated in tumour-derived extracellular vesicles (TDEV). These vesicles can enhance the susceptibility of tumour cells to viral oncolysis and, via a synthetic lethality approach, can also sensitise tumour cells to small molecule inhibitors (9).

Here we show that virally induced TDEV are preferentially taken up by myeloid cells, including TAMs, making TAMs an ideal target for this approach. Notably, numerous miRNAs have been reported to drive TAM polarisation (13) making miRNA reprogramming an attractive strategy to alter TAM function. However, developing effective strategies for delivery of miRNAs into TAMs is essential for the development of effective miRNA therapeutics. In this regard, OVs preferentially replicate in tumour cells and also enhance TDEV production making them ideal vehicles to deliver miRNA to the TME (9).

In this study we have identified two miRNA, miR-155 and miR-19a, that regulate the TAM phenotype and delivered them to the TME using ORV vectors. This miRNA delivery limits the immunosuppressive activity of TAMs enhancing antigen presentation and supporting anti-tumour T cell responses. While ORV-miR-155 demonstrates some control of OvCa tumour growth, ORV-miR-19a induces long-term survival of mice bearing ID8*Trp53*$^{-/-}$ tumours, suggesting that ORV-miR19a might prove an effective, novel cancer immunotherapy for the treatment of OvCa.

Results

ORV enhances the production of TDEV from OvCa cells *in vitro* and *in vivo*

Previously, we demonstrated that ORV infection enhances secretion of TDEV from pancreatic and renal cancer cells (9). We wanted to confirm whether this was also true for human and mouse OvCa cells following ORV infection. Three human OvCa cell lines were infected with either ORV, ORV expressing a non-targeting control miRNA (ORV-miR-NTC), a single replication-cycle ORVΔG or PBS control. TDEVs were collected 24 h following infection and expression of AliX, TSG101 and CD9 were determined by immunoblot analysis (Figure 1A). To assess the production of TDEVs in the murine OvCa cell line, ID8*Trp53*$^{-/-}$, cells were infected with PBS or ORVΔG. TDEVs were collected, and concentration was determined using nano-tracking analysis (NTA) (Supplementary Figure S1A; n=1). Demonstrating, as per our previous findings in pancreatic and renal cells, that ORV/ORVΔG infection can enhance the production of TDEV from human and mouse OvCa cells. Furthermore, using NTA, we were also able to establish that whilst ORVΔG infection increased the abundance of TDEV, the average size of the vesicles remained unchanged (93.2nm [PBS] vs 91.8nm [ORVΔG]). To establish whether the increased production of TDEV could also be detected *in vivo*, ORV was administered to mice bearing intra-peritoneal ID8 tumours. 48h following ORV treatment, mice were sacrificed, peritoneal lavage performed and the concentration of TDEV assessed using a sandwich ELISA against two tetraspanin molecules, CD63 and CD81, that are located in the membranes of TDEV (Figure 1B). Following ORV treatment, the number of TDEV detected in the peritoneal cavity of ID8 bearing animals was significantly increased, confirming that the increase in TDEV is not just limited to infection of *in vitro* cultured cell lines but also occurs *in vivo*.

TDEV are preferentially taken up by myeloid-lineage immune cell populations

To determine which immune cell types, present in the TME could be targeted by ORV-induced TDEV-miRNA, we investigated the uptake of TDEV by human peripheral blood mononuclear cells (PBMCs). TDEV were collected from ascitic fluid from five OvCa patients and characterised by cryo-electron microscopy (Supplementary Figure S1B), TDEV were then fluorescently labelled with PKH-26 and cultured with PBMC overnight. TDEV uptake by monocytes (CD14+), T cells (CD3+CD56-), Natural killer (NK) cells (CD3-CD56+) and B cells (CD19+) was determined by flow cytometry. The vast majority of TDEV were taken up by CD14+ monocytes and a small number by B cells, while T and NK cells did not display any PKH-26 positivity, indicating no TDEV uptake (Figure 1C). To determine the efficiency of TDEV uptake by monocytes, a range of TDEV concentrations was investigated, based on either the initial ascitic volume they were isolated from or by a known concentration of TDEV isolated from SKOV-3 cells (Supplementary Figures S1C, D). These results demonstrate a dose dependent increase in TDEV uptake. Moreover, to determine the relative uptake of TDEV when tumour cells were present, PKH-26 labelled TDEV were added to tumour:PBMC co-cultures, and the percentage of TDEV positive tumour (CD45-) and CD14+ cells was assessed using flow cytometry (Figure 1D). The proportional uptake of TDEV by tumour cells and CD14+ cells was 40% and 60%, respectively, indicating that TDEV uptake by myeloid cells still occurs in the presence of tumour cells. Finally, to confirm TDEV uptake by murine TAMs as well as human TAMs, TDEV isolated from ID8*Trp53*$^{-/-}$ were fluorescently labelled with PKH-26 and cultured with freshly isolated peritoneal cells from ID8*Trp53*$^{-/-}$ tumour bearing mice. TDEV uptake was quantified by flow cytometry and revealed that virtually all F4/80+ macrophages were positive for PKH-26 labelled TDEV (Figure 1E). These results indicate that myeloid populations within the TME could be targeted with ORV expressing miRNA to reverse their tumour promoting phenotype.

In vitro generated TAMs have similar phenotypic and functional activities as TAMs isolated from ascitic fluid of ovarian cancer patients

Patient samples can be challenging to obtain regularly. Therefore, to study the tumour promoting features of human TAMs, we generated TAMs by co-culturing PBMC with tumour cells, to mimic how these immunosuppressive cell populations are

10.3389/fimmu.2024.1500570

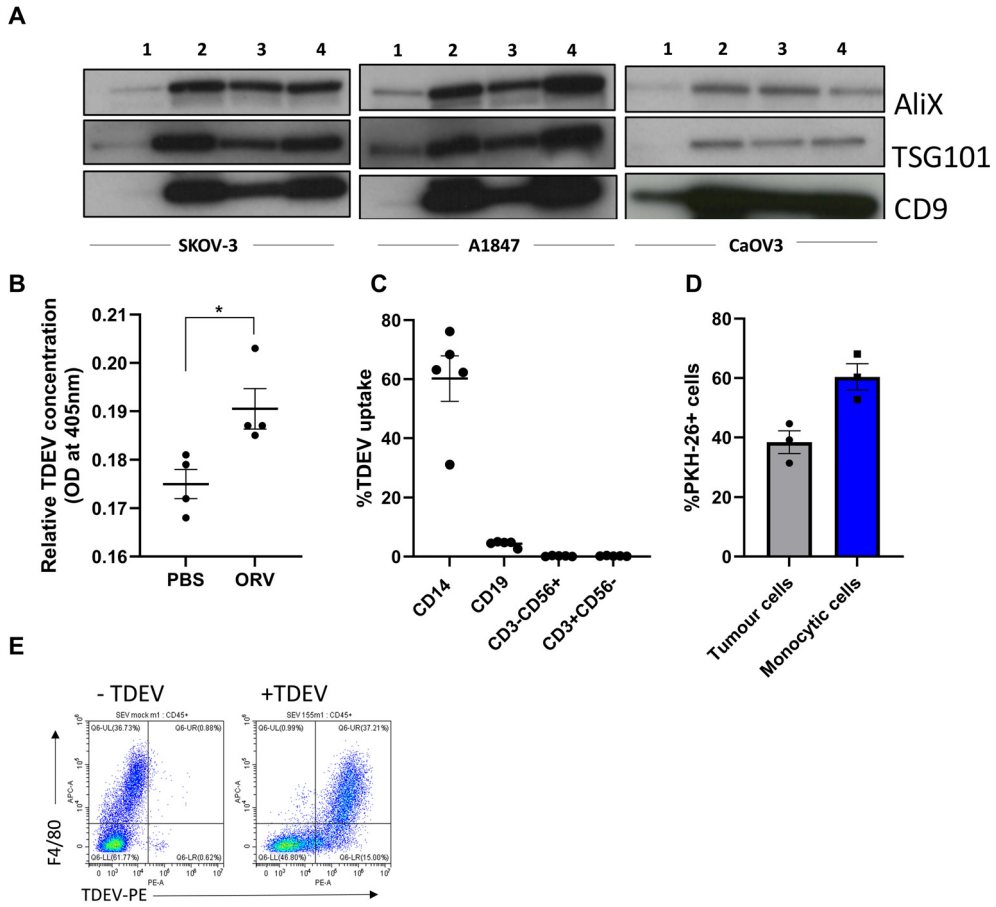

FIGURE 1
Production and uptake of TDEV following ORV infection of OvCa cells. **(A)** TDEV were collected from the supernatants of SKOV-3, A1847 and CaOV3 cells following 24 h treatment with either PBS (1) ORV (2), ORV-miR-NTC (3) or ORVΔG (4) and immunoblot analysis performed against ALiX, TGS101 and CD9 (n=3), one representative blot is shown. **(B)** ELISA quantification of EVs isolated from the peritoneal of ID8 bearing animals 48 h following treatment of PBS or ORV (n=3), a Mann-Whitney Test was performed *p<0.05. **(C)** The percentage uptake of PKH-26 labelled TDEV (isolated from five malignant OvCa ascites) in monocytes (CD14+), B (CD19+), T (CD3+CD56-) and NK (CD3-CD56+) cells determined by flow cytometry. **(D)** The percentage uptake of PKH-26 labelled TDEV in tumour (CD45-) and monocytes (CD45+ CD14+) in tumour:PBMC co-cultures (n=3) determined by flow cytometry. **(E)** Dot plot showing the uptake of PKH-26 labelled murine TDEV in peritoneal macrophages (F4/80+) by flow cytometry.

generated in human disease (rather than using recombinant cytokines). PBMC were cultured with either SKOV-3 or OVCA433 OvCa cells for seven days at a 50:1 ratio. CD14+ cells were isolated, and the immunosuppressive phenotype and function of CD14+ cells were tested alongside CD14+ cells isolated from OvCa patients. Cell surface staining of macrophage markers CD163 and CD206 on *in vitro* generated TAMs verses monocytes was initially evaluated by flow cytometry. Day seven generated CD14+ TAMs expressed both CD163 and CD206, similar to freshly isolated patient-derived TAMs, whereas PBMC-derived monocytes without tumour co-culture did not express either CD163 or CD206; moreover, during TAM generation, CD14+ cells became more granular, consistent with a pro-tumour phenotype, as assessed by an increase in side-scatter (SSC) upon flow cytometry acquisition (Figure 2A). Expression of PD-L1, B7-H4, and Arginase 1 have all been reported to be expressed on TAMs isolated from OvCa patients (14, 15). Therefore, expression of these molecules was also evaluated on CD206+CD163+ cells. TAMs generated from either SKOV-3 or OVCA433 co-cultures expressed high levels of cell-surface PD-L1 and B7-H4 (Figure 2B), and Arginase 1 expression was confirmed by intra-cellular staining (Figure 2C), while expression on pre-cultured monocytes was not observed (data not shown). Next, quantitative PCR was performed to evaluate the expression of the pro-tumour TAM-associated genes *IL-10*, *CCL2* and *IDO-1*, which were all increased in both SKOV-3 and OVCA433 generated TAMs compared to pre-cultured autologous monocytes (Figure 2D). To determine if *in vitro* generated TAMs were functionally immunosuppressive, TAMs were co-cultured with CD14- PBMCs at a ratio of 10:1, and the ability of T cells to proliferate following CD3/CD28 stimulation was assessed by tritiated thymidine. Importantly, *in vitro* generated TAMs significantly inhibited T cell proliferation, to similar levels observed with TAMs isolated from OvCa patient samples (Figure 2E). Finally, to determine if these *in vitro* generated

10.3389/fimmu.2024.1500570

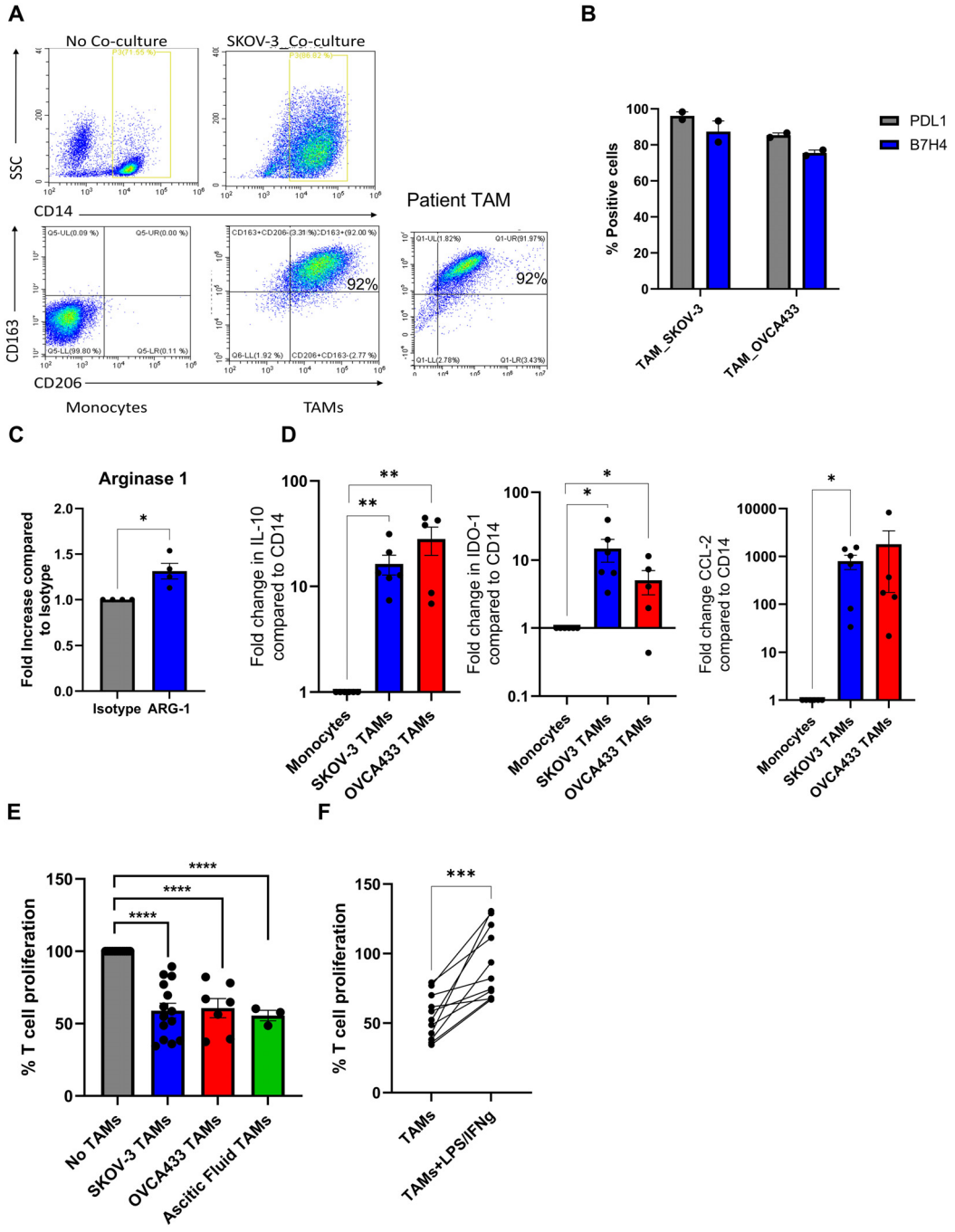

FIGURE 2
Characterisation of *in vitro* generated TAMs and TAMs isolated from OvCa patients. **(A)** Representative dot plots of autologous monocytes *vs* day 7 TAMs and OVCA patient ascitic fluid TAM displaying forward *vs* side scatter and CD163 and CD206 cell surface expression on CD14+ monocytes determined by flow cytometry. **(B)** PD-L1 and B7-H4 cell surface expression on Day 7 TAMs (CD14+) generated from SKOV-3 and OVCA433 co-cultures determined by flow cytometry (n=2). **(C)** Relative intra-cellular Arginase-1 expression compared to isotype control in SKOV generated TAMs was determined by flow cytometry (n=4), a unpaired T Test was performed *p<0.05 **(D)** Fold change calculated by (2^-ΔΔCT) method of *IL-10*, *IDO-1* and *CCL2* expression in TAMs generated from SKOV-3 and OVCA433 compared to autologous pre-co-cultured monocytes determined by qPCR (n=5), unpaired T Tests were performed (*p<0.05; **p<0.01). **(E)** Percentage of T cell proliferation following five days stimulation with CD3/CD28 Dynabeads cultured with, no TAMs, *in vitro* generated TAMs [SKOV3 (n=14) and OVCA433 (n=7)] or patient-derived TAMs (n=3) using tritiated thymidine, a one-way ANOVA was performed ****p<0.001). **(F)** Same as **(E)** but with SKOV-3 generated TAMs± LPS/IFNγ treatment prior to T cell co-culture (n=11), an unpaired T Test was performed ***p<0.005.

10.3389/fimmu.2024.1500570

TAMs could be reprogrammed to a less immunosuppressive anti-tumour phenotype, TAMs were treated with LPS/IFNγ overnight and co-cultured with T cells for four days prior to assessment of T cell proliferation; LPS/IFNγ treatment significantly alleviated TAM suppression of T cell proliferation (Figure 2F). These results demonstrate that TAMs can be generated *in vitro* using OvCa: PBMC co-cultures and confirm that *in vitro* generated TAMs retain plasticity for reprogramming when provided with polarising stimulus.

Dysregulation of miRNA expression occurs during macrophage polarisation

To identify miRNA that are dysregulated during pro-tumour and anti-tumour TAM polarisation, we performed small RNA sequencing on *in vitro* SKOV-3 generated TAMs ± LPS/IFNγ and autologous monocytes from four donors. Small RNA sequencing revealed several differentially expressed (DE) miRNAs following TAM differentiation; a total of 101 miRNAs were downregulated and 170 were upregulated by greater than 2-fold compared to monocytes (Figure 3A; left panel). While TAMs cultured with LPS/IFNγ overnight resulted in 15 miRNAs being downregulated, and 23 miRNAs upregulated by greater than 2-fold (Figure 3A; right panel). As TAMs treated with LPS/IFNγ are less suppressive (Figure 2F), we initially focussed on these 23 upregulated miRNAs, which are depicted in a heatmap showing the relative expression of miRNAs in TAM and TAM+LPS/IFNγ (Figure 3B). Next, we compared the expression of these up- and down-regulated DE-miRNA in each condition. Figure 3C shows a Venn diagram of the up- and down-regulated DE miRNA identified in Figure 3A. Of the 23 miRNA that were significantly upregulated in TAM+LPS/IFNγ, 4 were also significantly upregulated in TAMs compared to monocytes, and 3 were significantly upregulated in TAM+LPS/IFNγ and monocytes compared to TAMs, leaving 16 that were exclusively upregulated in TAM+LPS/IFNγ compared to TAM. Of these 16, miR155-5p was the most abundant miRNA upregulated in LPS/IFNγ treated TAMs (Figure 3D). To validate the small RNA sequencing, we measured miR-155-5p expression in *in vitro* generated TAMs ± LPS/IFNγ from an additional 5 donors, and patient TAMs± LPS/IFNγ (Figure 3E); this confirmed that miR-155-5p was significantly induced following LPS/IFNγ treatment. Multiple studies have identified miR-155-5p as a key miRNA implicated in driving TAM polarisation towards an anti-tumour phenotype (16–19), therefore, we cloned miR-155 into ORV and ORVΔG to determine if re-introducing this miRNA could improve anti-tumour responses compared to ORV-miR-NTC. Importantly, assessment of the oncolytic activity of ORV-miR-155 (compared against ORV-expressing GFP or miR-NTC control; Supplementary Figure S1) using two human OvCa cells lines (SKOV-3 and OVCA433) and the murine OvCa cell line ID8*Trp53*$^{-/-}$ demonstrated that miR-155 (or control miRNA) did not alter the cytotoxic capacity of ORV as there was no significant difference in OvCa cell death compared to ORV-GFP.

TDEV containing virally expressed miR-155 reverse the suppressive activity of TAMs

Having confirmed the oncolytic activity of ORV-miR-155 was not affected by expression of miR-155, we investigated whether TDEV containing miR-155 could modulate TAM immunosuppressive activity. To ensure our TDEV were not contaminated with ORV particles, ORVΔG-GFP-miRNA (single cycle-replication defective viruses) were used to generate TDEV-miRNA, as per our previous studies (9),TDEV preparations were routinely checked for and found to be free from viral contamination. Firstly, expression levels of the mature miR-155-5p were quantified in SKOV-3 TDEV following infection with either mock (PBS), ORVΔG-miR-NTC or ORVΔGmiR-155, relative to RNU6 control (Figure 4A). miR-155-5p expression was significantly elevated in TDEV following ORVΔ-miR-155 infection compared to ORVΔG-miR-NTC. Next, we tested the potential of TDEV containing miR-155 to reverse the suppressive activity of TAMs. TDEV were isolated from SKOV-3 conditioned medium following infection of ORVΔG-miR-155 or -miR-NTC and co-cultured with *in vitro* generated or patient derived TAMs overnight before being used in a T cell proliferation assay. T cells that had been cultured with *in vitro* generated TAMs + TDEV-miR155 were significantly less suppressive than TAMs receiving any of the control treatments (Figure 4B). Furthermore, TAMs isolated from one patient ascites fluid also demonstrated reduced immunosuppressive activity when treated with TDEV-miR155 (Supplementary Figure S4). These results demonstrated the overall utility of our approach and suggest that TDEV derived from ORVΔG-miR-155 infected cells had the capacity to reduce the immunosuppressive activity of TAMs.

ORV-miR155 enhances expression of antigen presenting genes in TAMs and enhances T cell responses *in vivo*

Next, we determined if TDEV containing miR-155 were functional in murine TAMs. Murine TAMs were generated by culturing bone marrow macrophages with ID8 conditioned medium for 48 h. Knockdown of miR-155 target genes, *Socs-1*, *Arginase-1* and *-2* was assessed by qPCR and Arginase-1 protein expression determine by intra-cellular flow cytometry. miR-155 targets were decreased in TAMs at both the mRNA and protein level following TDEV-miR-155 compared to controls (Figures 5A, B). Taken together these results suggest that TDEV from OvCa cells infected with ORVΔG-miR-155 are functional in both human and mouse TAMs. Having established *ex vivo* functionality, the ability of ORV-miR155 to modulate TAM function *in vivo* was investigated using animals bearing ID8Trp53$^{-/-}$OVA in order to track and measure SIINFEKL antigen responses. As miR-155 has previously been reported to enhance antigen presentation, expression of MHC-I and MHC-II on peritoneal macrophages was investigated. Expression of I-Ab (MHC-II) and H-2K^{b}-SIINFEKL (MHC-I-SIINFEKL) on F4/

10.3389/fimmu.2024.1500570

80+ cells were evaluated by flow cytometry following a single dose of either ORV-miR-NTC or ORV-miR155 to ID8*Trp53*$^{-/-}$OVA bearing animals. Following ORV-miR-155, F4/80+ cells expressed significantly more I-Ab (Figure 5C) and H-2K^{b}-SIINFEKL complexes (Figure 5D) compared to control virus, suggesting that TAMs were better able to present tumour-associated antigens to T cells. Next, we evaluated the anti-OVA T cell responses generated from ID8*Trp53*$^{-/-}$OVA bearing animals following three doses of either PBS, ORV-miR-NTC or ORV-miR-155. Splenocytes were isolated, stimulated *ex vivo* with SIINFEKL and concentration of

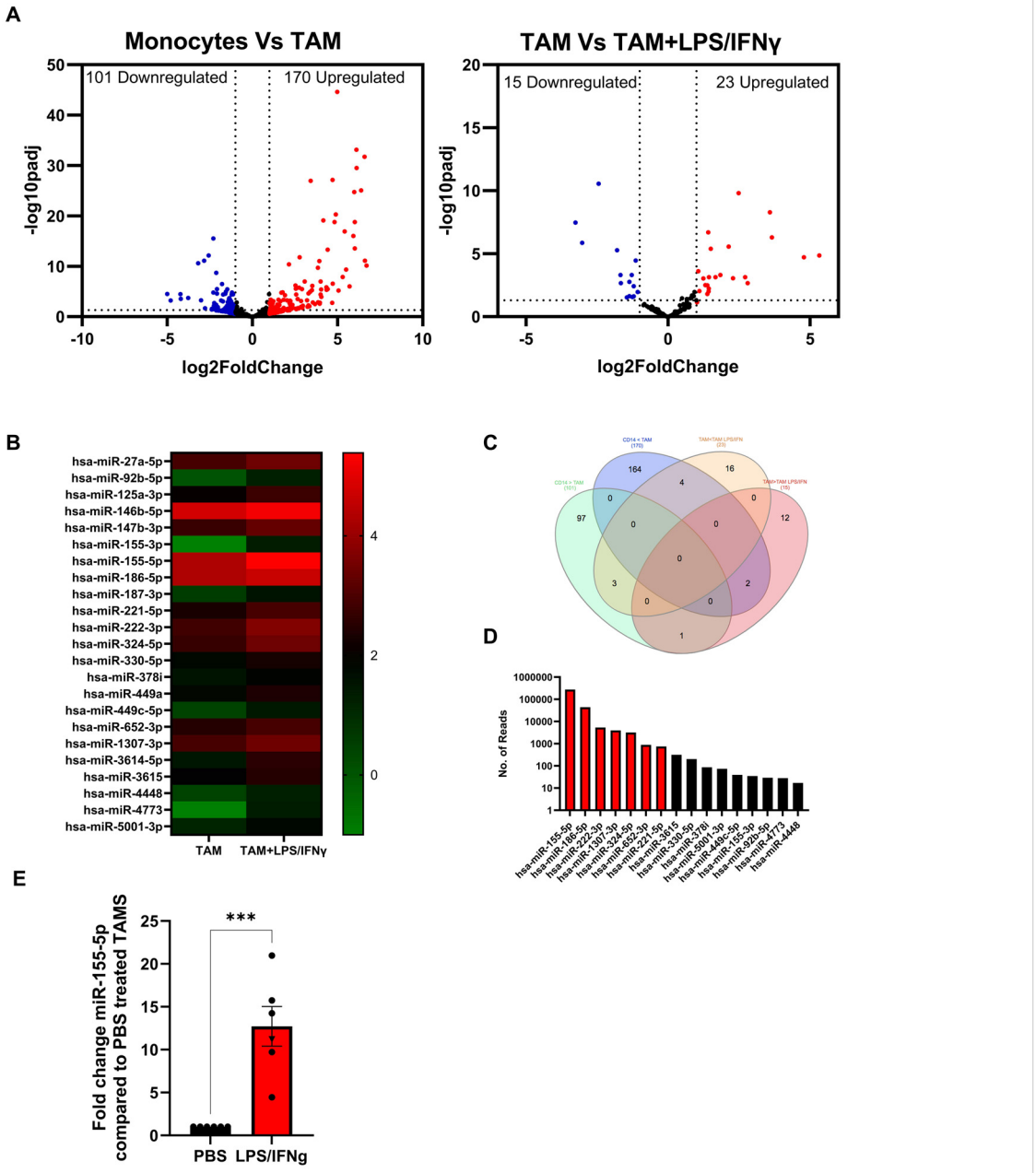

FIGURE 3
Identification of dysregulated miRNA expression in *in vitro* generated TAMs. Small RNA sequencing on *in vitro* SKOV-3 generated TAMs ± LPS/IFNγ and autologous monocytes from four donors was performed. **(A)** Volcano plots of differentially expressed miRNA in (i) Monocytes vs TAM or (ii) TAMs vs TAM+LPS/IFNγ; each dot represents a miRNA (red indicates the miRNAs that are upregulated two-fold while the blue indicates the miRNAs that are downregulated two-fold). The x-axis and y-axis are the log2 (fold change) and base mean expression values, respectively (n=4). **(B)** Heat map of the mean log^{10} expression of the 23 significantly upregulated miRNA in TAMs treated with LPS/IFNγ compared to untreated TAMs (n=4). **(C)** Venn diagram of the distribution of miRNA significantly up or down regulated by 2-fold in each of the comparisons. **(D)** Mean absolute reads for the 16 miRNA that are expressed greater in TAM+LPS/IFNγ compared to monocytes and TAMs. **(E)** Fold change in expression of miR-155-5p in five *in vitro* generated TAM (circles) and one patient TAM (Triangle) following LPS/IFNγ treatment compared to PBS control, an unpaired T Test was performed ***p<0.005.

10.3389/fimmu.2024.1500570

IFNγ assessed by ELISA (Figure 5E). Encouragingly, splenocytes from ORV-miR-155 treated mice secreted significantly greater concentrations of IFNγ compared to control virus indicating that expression of miR-155 from ORV enhanced the generation of OVA-specific T cells. To establish if this enhanced generation of tumour specific T cells resulted in improved survival, ID8*Trp53*$^{-/-}$OVA bearing animals were treated with the same treatment schedule and then monitored for ascites development. The median survival of ID8*Trp53*$^{-/-}$OVA-bearing animals treated with ORV-miR-155 was 46 days compared to 40 days for ORV-miR-NTC treated animals (Figure 5F) demonstrating improved tumour control over PBS treatment groups (median survival=33 days). However, the statistical significance between ORV-miR-NTC and ORV-miR155a was not reached (p=0.07).

ORV-miR19a significantly improves survival for ID8 bearing animals

We next, postulated whether restoring a miRNA lost during TAM differentiation, rather than targeting a miRNA modulated by LPS/IFNγ, would provide an alternative, potentially more potent, effect on macrophage function. miR-19a was one of the most abundant miRNAs that was significantly downregulated in TAMs generated from SKOV-3 culture compared to CD14+ monocytes. Moreover, as miR-19a has previously been implicated in reversing TAM function in a breast cancer model and has also been reported to be downregulated in TAMs isolated from GBM patients (20, 21), we sought to investigate whether targeting down regulated miRNA would be a more efficacious approach. Expression levels of miR-19a-3p were therefore investigated in TAMs generated from another OvCa cell line, OVCA433 alongside SKOV-3, to confirm sequencing results (Figure 3). TAMs generated from both cell lines demonstrated a significant reduction in miR-19a-3p expression (Figure 6A). Furthermore, when miR-19a-3p expression was measured in CD11b+ cells isolated from ID8 bearing animals and compared to non-tumour bearing animals (Figure 6B), a significant reduction in miR-19a-3p was observed compared to controls. The ability of TDEV-expressing miR-19a-3p to modulate TAM function was next assessed using T cell proliferation assays. Similar to results obtained with miR-155, expressing miR-19a from ORV did not enhance (or abrogate) ORV cytotoxicity (Supplementary Figure S2), but TDEV containing miR-19a (Figure 6C) significantly reduced the suppressive nature of TAMs on T cell proliferation (Figure 6D). Finally, to determine if ORV-miR-19a was effective at improving survival of mice bearing OvCa tumours, ID8*Trp53*$^{-/-}$ bearing animals were treated with either PBS, ORV-miR-NTC or ORV-miR-19a and monitored for the formation of ascites. ORV-miR-19a treatment significantly improved the survival of ID8*Trp53*$^{-/-}$ bearing animals compared to control virus and PBS treatment (Figure 6E). Taken together, these results demonstrate the ability of miR-19a expression in combination with ORV to generate potent anti-tumour immune responses in OvCa. The overall proposed mechanism of action of this approach is illustrated in Figure 7.

Discussion

TAMs are the most abundant immunosuppressive cell within the TME of HGSOC patients and play a critical role in generating and

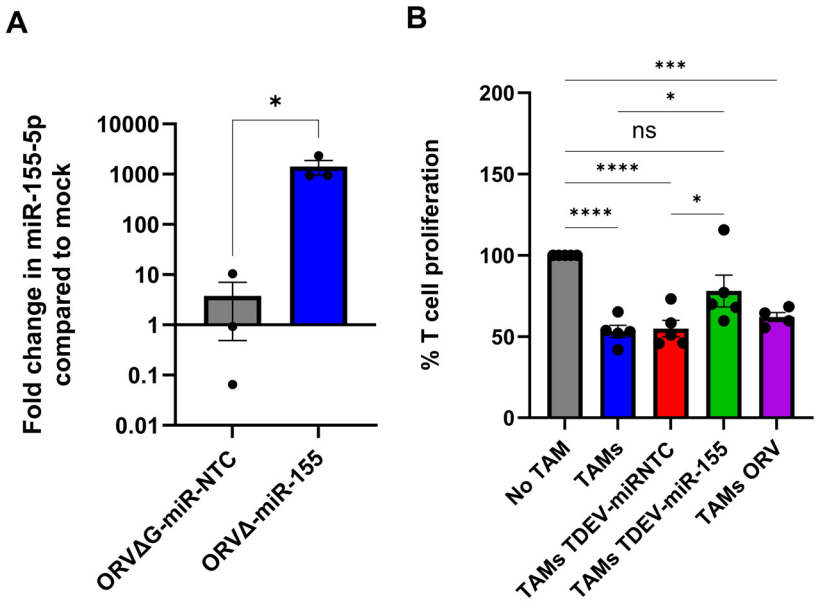

FIGURE 4
Characterisation of TDEV-miR-155 on *in vitro* generated TAM. **(A)** Shows the fold change in miR-155-5p expression in TDEV isolated following infection of SKOV-3 cells with ORVΔG-miR-155 and ORVΔ-miR-NTC compared to uninfected controls determined by qPCR (n=3), an unpaired T Test was performed *p<0.05. **(B)** Percentage of T cell proliferation (via tritiated thymidine incorporation) following five days stimulation with CD3/CD28 Dynabeads cultured with, no TAMs, SKOV3 *in vitro* generated TAMs either co-cultured with TDEV-miR-NTC, TDEV-miR-155 or ORV overnight prior to T cell co-culture (n=5) a one-way ANOVA was performed *p<0.05; ***p<0.005; ****p<0.001; ns, not significant.

10.3389/fimmu.2024.1500570

maintaining an immunosuppressive niche, providing a significant obstacle for effective anti-cancer therapies, including cancer immunotherapies. Over the last decade it has become clear that miRNA expression can play a pivotal role in macrophage polarisation by simultaneously regulating the expression multiple cellular targets (18). This coordinated biological response induced by miRNA makes them an attractive strategy to reprogramme TAMs. However, understanding the intricate regulatory networks involved in TAM polarisation, as well as developing effective strategies to re-introduce miRNAs into TAMs, is essential for the development of

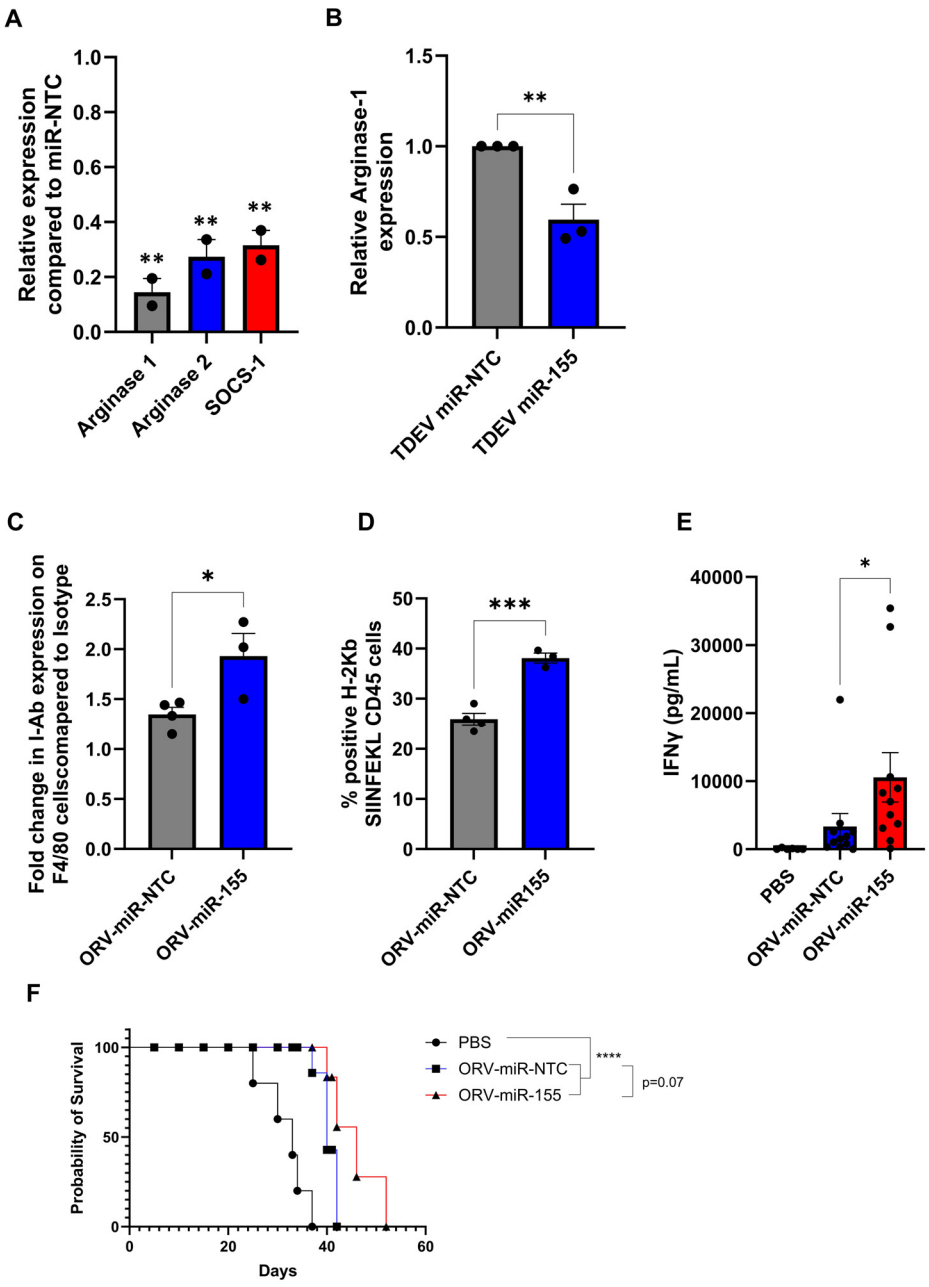

FIGURE 5
Investigating the efficacy of ORV-miR-155 in tumour bearing animals. **(A)** Fold change of miR-155-5p target genes *arginase-1*, *arginase-2* and *socs-1* in murine TAMs following incubation with TDEV-miR-155 compared to TDEV-miR-NTC determined by qPCR, a unpaired T Test was performed **p<0.01 **(B)** Relative intra-cellular Arginase-1 expression in murine TAMs treated with TDEV-miR-155 compared to TDEV-miR-NTC (n=3) by flow cytometry a unpaired T Test was performed *p<0.05. C57Bl/6 mice were intra-peritoneally injected with 5e6 ID8*Trp53*$^{-/-}$OVA cells, seven days post tumour seeding mice were treated with one **(C, D)** or three doses **(E, F)** (every other day) with ORV-miR-155 (1e8 PFU), ORV-miR-NTC (1e8 PFU) or PBS control. **(C, D)** Peritoneal lavage was performed 48 h post virus infection and cell surface expression of I-Ab **(A)** and H2-Kb-SIINFEKL **(B)** on F4/80+ cells was determined by flow cytometry; unpaired T Tests were performed *p0<.05; ***p<0.005. **(E)** Spleens were collected from mice five days post last viral injection. Splenocytes were stimulated ± SIINFKEL (5 ug/ml) for 48 h. The concentration of IFNγ in the cell-free supernatant was determined by ELISA (n= 6 PBS; n=11 ORV-miRNA) a Mann-Whitney Test was performed *p<0.05). **(F)** Kaplan-Meier survival curve of treated animals (5 mice/group) a Mantel-Cox Test was performed ****p<0.0001.

10.3389/fimmu.2024.1500570

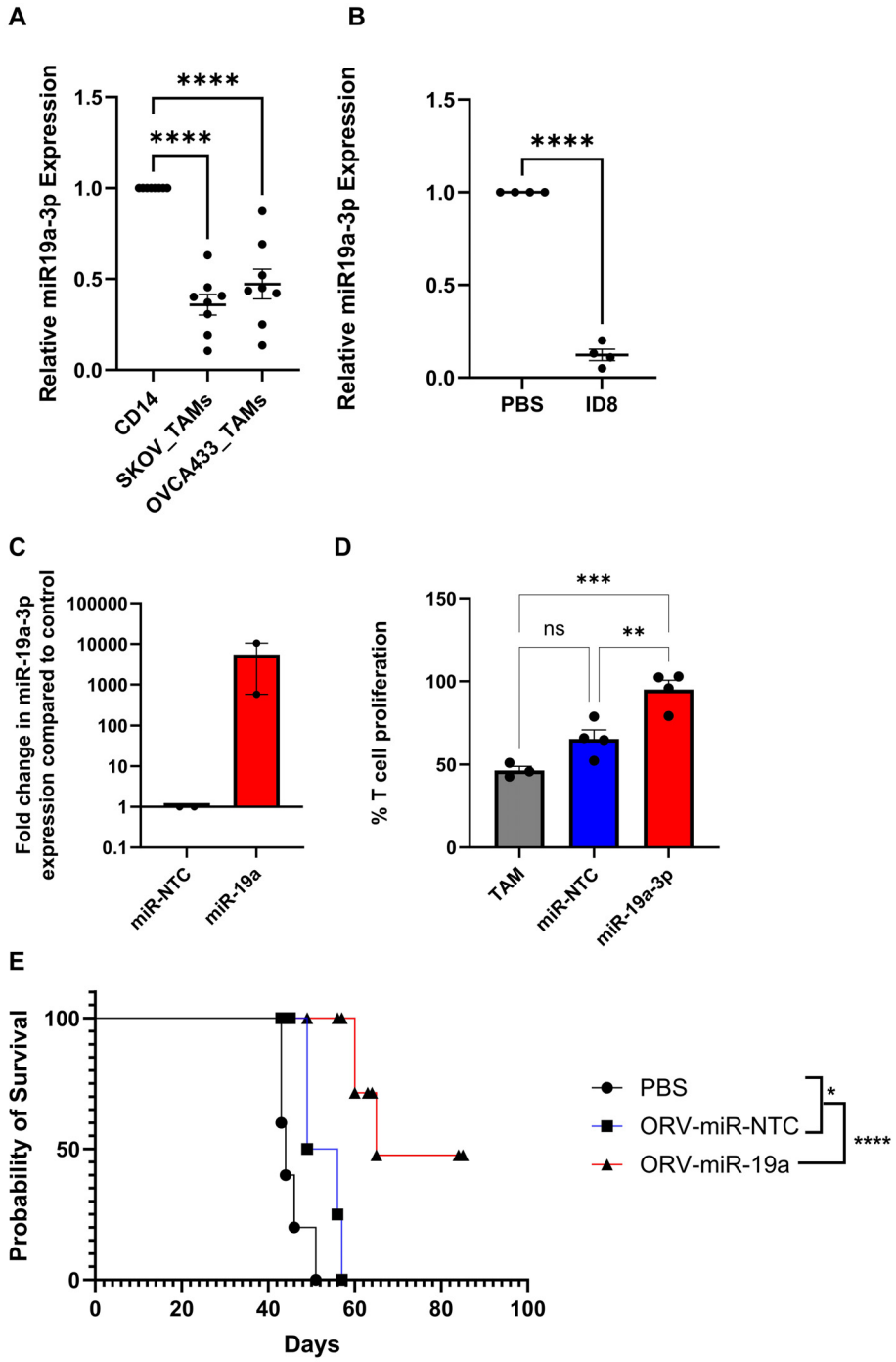

FIGURE 6
Restoring miR-19 expression in TAMs elevates T cell suppression and significantly improves survival of *ID8Trp53*$^{-/-}$ mice. A/B/C Relative expression of miR-19a-3p in **(A)** *in vitro* generated TAMs compared to autologous pre-cultured monocytes (n=8), one-way ANOVA was performed ****p<0.000, **(B)** CD11b+ cells isolated from ID8 bearing animals compared to non-tumour bearing animals (n=4), a unpaired T-Test was performed ****p<0.0001 or **(C)** TDEV used in **(D)** determined by qPCR (n=2). **(D)** Percentage of T cell proliferation (tritiated thymidine incorporation) following five days stimulation with CD3/CD28 dynabeads cultured with SKOV3 *in vitro* generated TAMs either co-cultured with PBS, TDEV-miR-NTC or TDEV-miR-19a overnight prior to T cell co-culture (n=4) one-way ANOVA was performed **p<0.001; ***p<0.0005; ns, not significant. **(E)** C57Bl/6 mice were injected i.p. with 5e6 ID8*Trp53*$^{-/-}$ seven days post tumour seeding mice received six doses (every other day) of either PBS, ORV-miR-NTC (1e8 PFU) or ORV-miR-19a (1e8 PFU) and monitored for ascites development. Kaplien-Meier survival curve of treated animals (5 mice/group) is shown, a Mantel-Cox test was performed *p<0.05; ****p<0.0001.

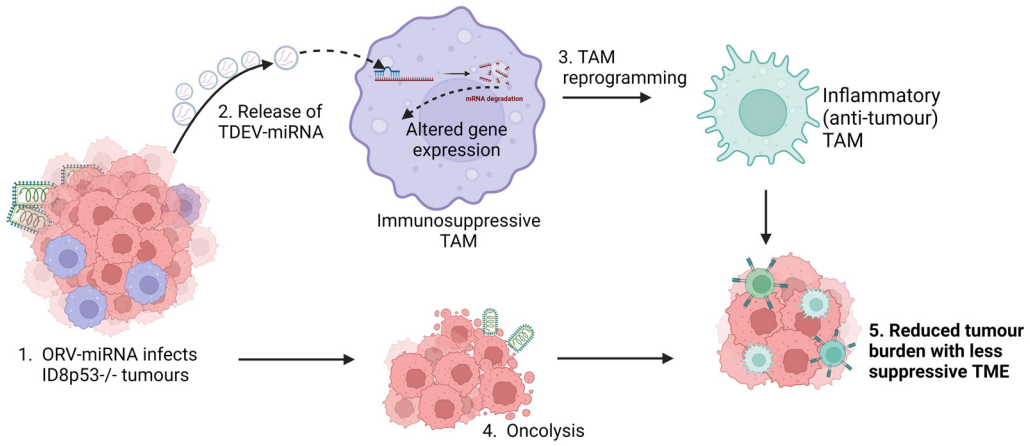

FIGURE 7
Schematic of overall proposed mechanism of action of ORV-miRNA. Following infection of tumour cells with ORV-miRNA, extracellular vesicles are released containing miRNA (TDEV-miRNA), followed by lysis of the tumour cells (oncolysis). Concurrently, TDEV-miRNA are taken up by tumour associated macrophages and are reprogrammed into a less suppressive, inflammatory (anti-tumour) phenotype, the exact mechanism of this altered gene expression is still under investigation. Critically, oncolysis together with TDEV-miRNA release reduces tumour burden and enhances anti-tumour immune responses in ID8 bearing animals.

effective miRNA therapeutics. As OVs specifically replicate within tumour cells, they are ideal vehicles to deliver transgenes into the TME. Our previous work showed that encoding artificial miRNA (amiRNA) into ORV resulted in virally encoded amiRNA in TDEV and that these vesicles could prime uninfected cells and sensitise them to small molecule inhibitors (7). We therefore hypothesised that we could use this same strategy to re-introduce therapeutic miRNA into other cells in the TME that are not intrinsically permissive to OV infection. Our preliminary studies identified that myeloid cells with the TME would be a suitable target cell for this approach as these cell populations readily take up TDEV. Previous publications have identified key miRNA that are associated with the differential polarisation states of TAMs (13, 22, 23). Specifically, in human TAMs, these have focussed on using the THP-1 monocyte cell line as a model system of primary monocytes with an artificial differentiation process (including PMA or individual cytokine treatment) (24). However, the THP-1 cell line may not fully exhibit the same plasticity as primary macrophages due to the genetic and epigenetic difference exhibited between the two cell types, and single cytokine treatments are artificial conditions unlikely to be encountered in the TME. Therefore, in this study we investigated whether we could generate TAMs by culturing human PBMC with tumour cells as we believed this would better recapitulate signalling more likely encountered in the TME. Here we show that co-culturing PBMC with tumour cells results in the generation of TAMs that display similar phenotype and function as TAMs isolated from ovarian cancer ascites. To identify which miRNAs to encode into our OV, small RNA sequencing was performed on these *in vitro* generated TAMs. These data revealed a number of miRNA molecules that displayed a greater than 2-fold difference in expression during TAM differentiation and anti-tumour stimulation, several of which have not previously been described to be involved in TAM polarisation. Consistent with other murine and human studies, the most abundant miRNA in LPS/IFNγ treated macrophages was miR-155-5p (23). miR-155-5p has been previously reported to be essential in the generation of anti-tumour immune responses and was therefore taken forward for further investigation (17). Our results show that ORV-miR-155 treatment induced enhanced anti-OVA T cell responses that resulted in some level of improved tumour control, although, no long-term cures were evident. Therefore, we hypothesised that an alternative approach that might be more efficacious, would be to reintroduce a miRNA downregulated during TAM differentiation. Sequencing revealed that miR-19a-3p was one of the top 10 abundant miRNAs expressed in monocytes that was significantly down-regulated in TAMs. Moreover, expression of miR-19a has also been reported to be significantly downregulated in GBM-associated TAMs and reverse the pro-tumour phenotype of TAMs in a murine breast cancer model (20, 21), therefore we next investigated the potential of this miRNA to enhance oncolytic virotherapy. ORV expressing miR-19 was able to enhance survival of ID8 bearing animals significantly and even resulted in several long-term cures. These results suggest that restoring miRNA that are lost in TAM differentiation may be more important than restoring miRNA that are upregulated in the anti-tumour phenotype. However, it is also feasible that expressing miR-19a within tumour cells alters TDEV composition and the effects seen in our study are an indirect consequence of altered gene expression within the TDEV producer cell line, further studies are ongoing to fully elucidate (i) the composition of TDEV +/-miR-19a and (ii) the mechanism of miRNA transfer into TAMs. This study also highlighted a further 100 miRNAs that were down regulated in TAMs, and it remains to be seen if TDEV expressing miR-19a is the most effective TDEV/miRNA to reverse the pro-tumour phenotype of TAMs or whether another TDEV containing miRNA may be superior. Studies are also ongoing to determine if encoding multiple miRNAs (e.g., miR-155 and miR-19a) into an OV or delivering different OV-miRNA sequentially improves therapy further. Sequential delivery will have to be appropriately timed to ensure that the induction of anti-viral immunity does not abrogate OV therapy; an alternative option could involve encoding different miRNA in

molecularly distinct viruses to ensure effective replication. Arming ORVs with immunomodulatory miRNA is an effective approach to overcome TAM-mediated immunosuppression within the TME and improve oncolytic virotherapy.

Materials and methods

Cell culture and reagents

SKOV-3, CaOV3 and Vero cell lines were purchased from ATCC. OVCA433 and A1847 were a gift from Dr. Sandra Bell, University of Leeds, UK. ID8*Trp53*$^{-/-}$ were provided by Dr. Iain McNeish, Imperial College London, UK. ID8*Trp53*$^{-/-}$OVA were a gift from Dr. Robert Salmond, University of Leeds, UK and T-REx^{TM}-293 cells were purchased from Invitrogen. All cell lines were routinely checked for mycoplasma and were free from contamination. SKOV-3, A1847 and OVCA433 were grown in glutamine-containing RPMI (Sigma-Aldrich Ltd). Vero, CaOv3, ID8*Trp53*$^{-/-}$, ID8*Trp53*$^{-/-}$OVA, were grown in glutamine containing DMEM (Sigma-Aldrich Ltd). T-RExTM-293 cells were cultured in glutamine containing DMEM, containing zeocin (300 µg/ml; Gibco) and blasticidin (5 µg/ml; *In vivo*gen).

PBMC were isolated from leukapheresis cones purchased from the NHS blood and transplant service. PBMC were isolated from whole blood by density gradient centrifugation on Lymphoprep (StemCell Technology®). PMBC were cultures with indicated tumour cells at a ratio of (50:1) for seven days to generate TAM. CD14^{+} cells were isolated from PBMC or PBMC/Tumour cell co-cultures using MACS isolation procedures, following the manufacturers' protocols (Miltenyi Biotec).

Ovarian cancer samples

Ovarian cancer patients undergoing routine paracentesis were identified and informed consent was given to collect ascitic fluid in accordance with local institutional ethics review and approval (REC approval no. 06/Q1206/106). Cells were pelleted by centrifugation at 450 x g for 10 min. Cells were collected for phenotypic analysis or function analysis following CD14 isolation. Supernatants were collected for EV isolation.

Viruses

The ORV used in this study was MG1, for which virus backbone and propagation protocols have previously been described (25). In brief, to construct and rescue the replication-competent miR-155, miR-19a and the NTC sequences were encoded into the pre-miR-30-based short hairpin cassette flanked with MLU-1 restriction (GenScript). Both miRNA-encoding plasmids and MG1 shuttle plasmids were digested using MLU-1 (NEB) and pre-miR-30-based cassette inserts were ligated individually into the MG1 shuttle vector, correct orientation of insert was confirmed by sanger sequencing. For single-cycle MRBΔG-GFP viruses (replication-defective), the infusion cloning technique was used to insert the miRNA sequences between the P-M genes, thus retaining GFP expression in between M-L genes. Firstly, a PCR amplification of the corresponding pre-miR sequences from GenScript plasmids was performed using the specific primers (forward primer: 5' AATATGAAAAAAACTCTCGAGGAAGGTATATTGCTG 3' reverse primer: 5' TTTGATATCTGTTAGGCTAGCCCGAGGCA GTAGGCA 3') followed by the PCR amplification of pMRBΔG-GFP (forward primer: 5' GCTAGCCTAACAGATATCAAAAG ATATCT 3' and reverse primer: 5' CTCGAGAGTTTTTTTCAT ATTCAAGCT 3'; all primers were purchased from Integrated DNA Technology). PCR products were then ligated in then In-Fusion® reaction (Takara). Positive colonies were confirmed by Sanger sequencing (Source Bioscience, Cambridge, UK). All viruses were rescued using an infection-transfection method as previously described (26). In the case of single-cycle viruses, MRBΔG viruses were rescued and titrated in T-REx^{TM}-293 cells expressing the G protein. T-REx^{TM}-293 cells containing a plasmid with doxycycline-inducible VSV G protein expression was used to produce the MRBΔG virus stocks. G protein expression was first induced with 800 µM doxycycline (DOX) and cells were immediately infected at MOI 0.05 in serum-free DMEM. After 2 h, the inoculum was removed and fresh DMEM with 10% FBS was added. After 24 h, medium was harvested, and large cellular debris was removed using a 2000 × g spin for 15 min at 4 °C. The medium was further cleared by filtering on a 0.22 µm SteritopTM filter unit (Millipore). Virus was pelleted (14,000 x g) for 1 h and stored at -80C.

Total RNA isolation, quantitative PCR, miRNA quantification, sequencing and analysis

RNA was extracted using TriZol following manufacturer's instruction (Invitrogen). RNA quantification and quality analysis was performed using Qubit Fluorometry HS kit (Thermo Fisher Scientific) and TapeStation (Thermo Fisher Scientific), respectively, according to manufacturer's instructions. For qPCR analysis 1ug of RNA was converted into cDNA using SuperScript V Reverse transcriptase (Invitrogen), quantification of genes was determined using matched primer pairs (Table 1) and SYBR green (QuantaBio) on QuantStudio 5 (Applied Bioscience). Small RNA sequencing was performed by Fasteris Life Science Genesupport, Switzerland using 20-500 ng of total RNA on Illumina-NextSeq 500 (1x75bp; 10-15 million reads per sample). Reads were mapped to the miRbase human reference database. DESeq2 R package was used to normalise the expected counts and perform the differential expression analysis.

Thymidine incorporation assay

TAMs were seeded at 2e4 cells/well in a flat-bottom 96-well plate, then treated with 6ug of TDEV from indicated sources overnight or with LPS/IFNγ (50ng/ml and 10ng/ml, respectively). The following day, CD14- PBMC were added to TAMs (or cultured alone) at a 10:1 ratio, then stimulated with CD3/CD28 Dynabeads as per manufacturer's instructions (Invitrogen). Three days later,

TABLE 1 List of primer sequences.

Gene	Forward sequence	Reverse sequence
Human IL-10	*5'-TTGCTGGAGGACTTT AAGGGTT-3'*	*5'-TCACATGCGCCTTG ATGTCT-3'*
Human IDO-1	*5'-ATGCAGACTGTGTC TTGGCA-3'*	*5'-GCGCCTTTAGCAAA GTGTCC-3'*
Human CCL2	*5'-GATCTCAGTGCAGA GGCTCG-3'*	*5'-TTTGCTTGTCCAGG TGGTCC-3'*
Human-RpIp0	*5'-TTAAACCCTGCGTGG CAATCC-3'*	*5'-CCACATTCCCCCGG ATATGA-3'*
Mouse Arg-1	*5'-GCTGAAGGTCTCTTC CATCACC-3'*	*5'-CATTGGCTTGCGAGAC GTAGAC-3'*
Mouse Arg-2	*5'-CACCTCTCACCACTGT ATCTGG-3'*	*5'-CCAGGAAAATCCTGGC AGTTGTG-3'*
Mouse SOCS-1	*5'-AGTCGCCAACGGAAC TGCTTCT-3'*	*5'-GTAGTGCTCCAGCAG CTCGAAA-3'*
Mouse- RpIp0	*5'-GCTTCGTGTCACCAAG GAGGA-3'*	*5'-GTCCTAGACCAGTG TTCTGAGC-3'*
miR-155-5p	*5'-TAATGCTAATCGTGATA GGGGT-3'*	*Universal primer*
miR-19a-3p	*5'-TGTGCAAATCTATGCA AAACTGA-3'*	*Universal primer*

tritiated thymidine (Revvity; 1μCi/well) was added and incubated at 37°C overnight. Cells were harvested onto a filtermat using a Cell Harvester FilterMate-96, and scintillation counts were acquired on 2450 Microplate counter, Microbeta^2 (Perkin Elmer).

Tumour derived extracellular vesicle isolation, quantification, and labelling

TDEV were collected using differential centrifugation of conditioned media or cell-free ascites. For conditioned media EVs, cells were infected at MOI 0.1 with MRBΔG viruses in serum-free media. After 2 h, medium was changed for RPMI with EV depleted serum and the cells were incubated for 24 h at 37°C. Samples were first subjected to 2000 × g for 10 mins to eliminate cells and cellular debris, followed by syringe filtration with 0.22um filter (Millpore). TDEVs were then pelleted using ultracentrifugation Beckman Coulter Optima L-100 XP Ultra- centrifuge at 120,000 × g for 1.2 h, washed in PBS and centrifuged again at 120,000 × g for 1.2 h; TDEV were resuspended in small volume or PBS. Quantification of TDEV was performed using the BCA assay kit (Pierce), Nanoparticle tracking and immunoblot analysis. Once isolated TDEV were labelled with either PKH-26 (Sigma) as per manufacturer's instructions.

Nanoparticle tracking analysis

To determine size distribution and concentration of TDEV preparations, Nanoparticle Tracking Analysis was carried out using a Nanosight NS300 (Malvern Panalytical, U.K.). TDEVs resuspended in 1× PBS were diluted 100- to 1000-fold. To ensure consistency in concentration readouts, measurements were performed using camera level 15 and analysis threshold 5. Samples were pumped across the detection window using a syringe driver set to 30 uL/minute in a 1mL syringe. NTA 3.4.4 software was used to determine the size distribution and concentration from five 60 second video loops per sample.

Immunoblotting analysis

TDEVs were harvested and lysed in RIPA buffer (25 mM Tris HCl pH 7.6, 150 mM NaCl, 1% NP-40, 1% sodium deoxycholate, 0.1% SDS) containing protease inhibitors (Roche). Cell lysates were clarified by centrifugation at 12,000 × g for 20 min at 4°C. Proteins were separated on Nupage® 4–12% Bis-Tris Protein Gels (Invitrogen) and transferred on polyvinylidene fluoride (PVDF) membranes (Immobilon-P Millipore, Bedford, MA) for 2 h or overnight at 4°C. Blocked membranes were incubated overnight at 4°C with the following diluted antibodies: ALIX (1:2000; Santa Cruz Biotechnology, sc-53538), CD9 (1:1000; Abcam, ab236630), TSG101 (1:1000; Abcam, ab125011).

Cryo-electron microscopy

Cryo-EM grids were prepared with 3 μl of purified EV preparation onto 200 mesh grids with 2-μm holes (Quantifoil R2/2, Quantifoil Micro Tools, GmbH, Germany). Grids were glow discharged for 30 s prior to applying the sample (Cressington, UK). Grids were plunge-frozen in liquid ethane cooled by liquid nitrogen using a FEI Vitrobot IV (FEI, The Netherlands) at 90% relative humidity, and a chamber temperature of 4°C. Micrographs were imaged using the FEI Titan Krios EM (Astbury Biostructure Laboratory, University of Leeds) at 300 kV, using a total electron dose of 60 e–/Å^2 and a magnification of ×75,000 and the EPU Software (Thermo Fisher). Micrographs were acquired using an energy-filtered K2 Summit direct electron detector (Gatan, USA), with a final object sampling of 1.07 Å/pixel.

Enzyme-linked immunosorbent assay

The production of murine IFNγ (R&D systems) in cell free supernatant was determined using matched-paired antibodies according to the manufacturer's instructions. To determine the abundance of extracellular vesicles in peritoneal lavages from mice treated ± MG1, equal volumes of lavage were used in a sandwich ELISA. Briefly, maxisorp plates (Nunc) were coated with mouse anti-CD63 (1:250) (R&D systems) overnight at 4°C, plates were then blocked for 2 h in PBS containing 10% FCS, the peritoneal lavages were added in triplicate and incubated overnight at 4°C. Plates were washed with PBS-Tween (0.05%) and mouse anti-CD81-Biotin (1:500) (Miltenyi biotec) added for 1 h at room temperature, washed PBS-Tween(3x), then incubated with Extravidin- alkaline phosphatase (Sigma; 1:5000) for 1 h before being washed PBS-Tween (3x) and then with dH_20 (3x) before the addition of substrate solution (1 mg/mL p-nitrophenyl phosphate)

in 0.2M TRIS buffer (both Sigma). Optical density absorbance readings were determined using a Thermo Multiskan EX plate reader (Thermo Fisher Scientific), at 405 nm absorbance.

Cell surface phenotyping

Cell surface expression of indicated markers were quantified by flow cytometry. Briefly, cells were harvested, washed in FACS buffer (PBS; 1% (v/v) FCS; 0.1% (w/v) sodium azide) and incubated for 30 mins at 4°C with specific antibodies or matching isotype controls. Cells were washed with FACS buffer and then fixed with 1% PFA (1% (w/v) paraformaldehyde in PBS) and stored at 4°C prior to acquisition. Flow cytometry analysis was performed either using CytoFLEX S or CytoFLEX LX (Beckman Coulter) and analysis carried out using CytExpert software.

Intra-cellular staining

Cells were cell-surfaced stained and fixed overnight with 1% PFA prior to permeabilisation with 0.3% Saponin (Sigma-Aldrich Ltd) for 15mins at 4°C. Cells were washed with 0.1% Saponin, incubated with specific antibodies or matched isotype controls for 30 mins at 4°C. Cells were wash with PBS and flow cytometry analysis was performed immediately using the CytoFLEX S.

Flow cytometry antibodies

All antibodies were purchased from BD Biosciences unless otherwise stated. Human CD14-FITC/BV421 (MφP9), CD19-FITC (4G7), CD3-PerCP (SK7), CD56-APC (NCAM16.2), CD45-APC (HI30), CD163-PE-CF594 (GHI/61), CD206-BV421 (19.2), mouse and human Arginase-1-FITC (R&D systems), PD-L1-FITC (MIH1), B7-H4-PE (H74) (eBioscience). Isotypes: Mouse IgG1 κ-PE (P3.6.2.8.1), Mouse IgG1, κ-FITC (MOPC-21) and Sheep IgG-FITC (R&D Systems). Mouse F4/80-APC (BM8) (BioLegend), I-Ab-FITC (AF6-120.1) and H2-Kb-SIINFEKL-PE (25-DI.16) (Biolegend); Isotypes Mouse IgG2a, κ-FITC (G155-178), Mouse IgG1, κ-PE (MOPC-21) (Biolegend).

Animals

Seven- to eight-week-old female C57Bl/6 mice (Charles River, UK) were selected for use in all *in vivo* experiments. These were conducted at the St. James's Biomedical Services, University of Leeds and were approved by the local Ethical Review Committee and standards of care were based upon the UKCCCR Guidelines for the welfare and use of animals in cancer research. Mice were injected i.p. with 5e6 ID8 cells (Wild type or *Trp53*$^{-/-}$ ± OVA) for 7 days then treated with PBS, ORV, ORV-miRNA-NTC, ORV-miR-155 or ORV-miR19a (1e8 PFU in 100uL PBS) every other day for three to six doses as indicated (5 mice/group), sample size was selected by performing power calculations based on previous experiments with wild type ORV, no animals were excluded from these studies, mice were randomised and all experiments were blinded to the veterinary staff performing procedures and monitoring the welfare of animals. The welfare of animals was monitored daily, and mice were sacrificed once ascites formation was confirmed.

Splenocyte recall assay

Spleens were immediately excised from euthanized mice and dissociated *in vitro* to achieve single-cell suspensions. Red blood cells were lysed with ACK lysis buffer for 1 minute. Cells were resuspended at 5×10^6 in glutamine containing RPMI containing 10% FCS. Splenocytes were cultured either alone or SIINFEKL peptide (5ug/mL). Cell-free supernatants were collected 48 hrs later and tested by IFNγ ELISA.

Statistical significance

Statistical analysis was carried out with the Graphpad Prism software, error bars show ± SEM. Statistical differences among groups were determined using student's t-test, one-way ANOVA or two-way ANOVA analysis.For survival experiments, the Kaplan-Meier survival curves were compared using log-rank (Mantel-Cox) test. Statistical significance was determined as follows: $*p<0.05$, $**p<0.001$, $***p<0.0001$ and $****p<0.0001$.

Data availability statement

The original contributions presented in the study are publicly available. This data can be found here: Gene Expression Omnibus (GEO), accession number GSE284314.

Ethics statement

The studies involving humans were approved by Leeds Teaching Hospital NHS trust in 2015, LTHR R&I number is CO06/7573 and the REC number is 06/Q1206/106. The studies were conducted in accordance with the local legislation and institutional requirements. The participants provided their written informed consent to participate in this study. The animal study was approved by UK home office and St. James's Biomedical Services, University of Leeds local Ethical Review Committee. following the UKCCCR Guidelines. The study was conducted in accordance with the local legislation and institutional requirements.

Author contributions

VJ: Conceptualization, Data curation, Formal analysis, Funding acquisition, Investigation, Methodology, Project administration, Resources, Software, Supervision, Validation, Visualization,

Writing – original draft, Writing – review & editing. RR: Data curation, Formal analysis, Investigation, Writing – review & editing. GM: Investigation, Writing – review & editing. TB: Investigation, Writing – review & editing. KR: Investigation, Writing – review & editing. NI: Investigation, Writing – review & editing. IS: Investigation, Writing – review & editing. SH: Investigation, Writing – review & editing. NA: Investigation, Writing – review & editing. DJ: Resources, Writing – review & editing. CR: Resources, Writing – review & editing. SB: Funding acquisition, Writing – review & editing. IM: Resources, Supervision, Writing – review & editing. JB: Conceptualization, Writing – review & editing. AM: Supervision, Writing – review & editing. CI: Conceptualization, Writing – review & editing. GC: Funding acquisition, Supervision, Writing – review & editing. FE: Funding acquisition, Supervision, Writing – review & editing.

Funding

The author(s) declare financial support was received for the research, authorship, and/or publication of this article. Ovarian Action funded VJ and RR-H and the consumables required to undertake this study. The CRUK grant DRCRPGTD funded AAM.

Acknowledgments

The authors would like to extend our sincere gratitude to Ovarian Cancer Action for their generous funding and support, which made this research possible. Their commitment to advancing ovarian cancer research, has been instrumental in enabling us to carry out this study. We would also like to thank Dr Robert Salmond and Dr. Sandra Bell for the kind gift of OvCa cell lines and their scientific input into this study.

Conflict of interest

The authors declare that the research was conducted in the absence of any commercial or financial relationships that could be construed as a potential conflict of interest.

Publisher's note

Supplementary material

The Supplementary Material for this article can be found online at: https://www.frontiersin.org/articles/10.3389/fimmu.2024.1500570/full#supplementary-material

SUPPLEMENTARY FIGURE 1
Characterisation of TDEV and uptake in monocytes. **(A)** TDEV were isolated from ID8*Trp53*$^{-/-}$ cells following 24 h treatment with PBS or ORVΔG and Nanoparticle Tracking Analysis performed, histograms showing the size distribution from both conditions (left; black line= mean distribution, red area= SD of five independent runs) and bar chart of particle concentration plotted (right). **(B)** Cryo-EM image of ascitc fluid isolated EVs. **(C)** The percentage uptake of PKH-26 labelled TDEV isolated from indicated starting volumes of malignant ascitic fluid (n=5) in CD14+ cells determined by flow cytometry. **(D)** The percentage uptake of fluorescently labelled TDEV isolated from SKOV3 culture media (0, 10 or 25 ug) in CD14 cells (n=3) determined by flow cytometry.

SUPPLEMENTARY FIGURE 2
The cytopathic effect of ORV is not altered with miRNA expression. The percentage of viable OvCa cells following treatment with increasing MOI (1-0.0001) of ORV-GFP, ORV-miR-NTC and ORV-miR-155 measured by MTT assay at 48h post-infection for SKOV-3 and 24 h post-infection for OVCA433 and ID8*Trp53*$^{-/-}$ cells (n=3).

SUPPLEMENTARY FIGURE 3
ORV-miR-NTC and ORV-miR-19a display the same cytopathic effect on OvCa cells. The percentage of viable OvCa cells following treatment with increasing MOI (1-0.0001) of ORV-miR-NTC and ORV-miR-19a measured by MTT assay at 48h post-infection for SKOV-3 and 24 h post-infection for OVCA433 and ID8*Trp53*$^{-/-}$ cells (n=3).

SUPPLEMENTARY FIGURE 4
The effect of TDEV-miR-155 treatment on patient derived TAMs. Percentage of T cell proliferation (via tritiated thymidine incorporation) following five days stimulation with CD3/CD28 Dynabeads cultured with, no TAMs, ascitic fluid isolated TAMs either co-cultured with TDEV-miR-NTC or TDEV-miR-155 overnight prior to T cell co-culture (n=1).

References

1. Available online at: https://targetovariancancer.org.uk/about-us/media-centre/key-facts-and-figures:~:text=Over%207%2C000%20women%20are%20diagnosed%20each%20year%20in,late%2C%20when%20the%20cancer%20is%20harder%20to%20treat.%E2%81%B5 (Accessed April 2024).

2. Xu Y, Spear S, Ma Y, Lorentzen MP, Gruet M, McKinney F, et al. Pharmacological depletion of RNA splicing factor RBM39 by indisulam synergizes with PARP inhibitors in high-grade serous ovarian carcinoma. *Cell Rep*. (2023) 42(10):113307. doi: 10.1016/j.celrep.2023.113307

3. Hamanishi J, Mandai M, Ikeda T, Minami M, Kawaguchi A, Murayama T, et al. Safety and antitumor activity of Anti-PD-1 antibody, nivolumab, in patients with platinum-resistant ovarian cancer. *J Clin Oncol*. (2015) 33(34). doi: 10.1200/JCO.2015.62.3397

4. Tong JG, Valdes YR, Sivapragasam M, Barrett JW, Bell JC, Stojdl D, et al. Spatial and temporal epithelial ovarian cancer cell heterogeneity impacts Maraba virus oncolytic potential. *BMC Cancer*. (2017) 17(1). doi: 10.1186/s12885-017-3600-2

5. Tong JG, Valdes YR, Barrett JW, Bell JC, Stojdl D, McFadden G, et al. Evidence for differential viral oncolytic efficacy in an *in vitro* model of epithelial ovarian cancer metastasis. *Mol Ther Oncolytics*. (2015) 2. doi: 10.1038/mto.2015.13

6. Jennings VA, Ilett EJ, Scott KJ, West EJ, Vile R, Pandha H, et al. Lymphokine-activated killer and dendritic cell carriage enhances oncolytic reovirus therapy for ovarian cancer by overcoming antibody neutralization in ascites. *Int J Cancer*. (2014) 134(5). doi: 10.1002/ijc.v134.5

7. Bourgeois-Daigneault M-C, Roy DG, Falls T, Twumasi-Boateng K, St-Germain LE, Marguerie M, et al. Oncolytic vesicular stomatitis virus expressing interferon-γ has enhanced therapeutic activity. *Mol Ther Oncolytics*. (2016) 3. doi: 10.1038/mto.2016.1

8. Alkayyal AA, Tai LH, Kennedy MA, De Souza CT, Zhang J, Lefebvre C, et al. NK-cell recruitment is necessary for eradication of peritoneal carcinomatosis with an IL12-expressing Maraba virus cellular vaccine. *Cancer Immunol Res*. (2017) 5(3). doi: 10.1158/2326-6066.CIR-16-0162

9. Wedge M-E, Jennings VA, Crupi MJF, Poutou J, Jamieson T, Pelin A, et al. Virally programmed extracellular vesicles sensitize cancer cells to oncolytic virus and small molecule therapy. *Nat Commun*. (2022) 13(1). doi: 10.1038/s41467-022-29526-8

10. Leone P, Buonavoglia A, Fasano R, Solimando AG, De Re V, Cicco S, et al. Insights into the regulation of tumor angiogenesis by micro-RNAs. *J Clin Med*. (2019) 8 (12):2030. doi: 10.3390/jcm8122030

11. Schoepp M, Ströse A, Haier J. Dysregulation of miRNA expression in cancer associated fibroblasts (CAFs) and its consequences on the tumor microenvironment. *Cancers (Basel)*. (2017) 9(12):54. doi: 10.3390/cancers9060054

12. Zhang B, Pan X, Cobb GP, Anderson TA. microRNAs as oncogenes and tumor suppressors. *Dev Biol*. (2007) 302(1):1–12. doi: 10.1016/j.ydbio.2006.08.028

13. Chatterjee B, Saha P, Bose S, Shukla D, Chatterjee N, Kumar S, et al. MicroRNAs: As critical regulators of tumorassociated macrophages. *Int J Mol Sci*. (2020) 21(19):1–22. doi: 10.3390/ijms21197117

14. Qu QX, Huang Q, Shen Y, Zhu YB, Zhang XG. The increase of circulating PD-L1-expressing CD68+ macrophage in ovarian cancer. *Tumor Biol*. (2016) 37(4). doi: 10.1007/s13277-015-4066-y

15. Kryczek I, Zou L, Rodriguez P, Zhu G, Wei S, Mottram P, et al. B7-H4 expression identifies a novel suppressive macrophage population in human ovarian carcinoma. *J Exp Med*. (2006) 203(4). doi: 10.1084/jem.20050930

16. Li X, Wang S, Mu W, Barry J, Han A, Carpenter RL, et al. Reactive oxygen species reprogram macrophages to suppress antitumor immune response through the exosomal miR-155-5p/PD-L1 pathway. *J Exp Clin Cancer Res*. (2022) 41(1). doi: 10.1186/s13046-022-02244-1

17. Zonari E, Pucci F, Saini M, Mazzieri R, Politi LS, Gentner B, et al. A role for miR-155 in enabling tumor-infiltrating innate immune cells to mount effective antitumor responses in mice. *Blood*. (2013) 122(2). doi: 10.1182/blood-2012-08-449306

18. Essandoh K, Li Y, Huo J, Fan GC. MiRNA-mediated macrophage polarization and its potential role in the regulation of inflammatory response. *Shock*. (2016) 46. doi: 10.1097/SHK.0000000000000604

19. Cubillos-Ruiz JR, Baird JR, Tesone AJ, Rutkowski MR, Scarlett UK, Camposeco-Jacobs AL, et al. Reprogramming tumor-associated dendritic cells *in vivo* using miRNA mimetics triggers protective immunity against ovarian cancer. *Cancer Res*. (2012) 72 (7):1683–93. doi: 10.1158/0008-5472.CAN-11-3160

20. Xu S, Wei J, Wang F, Kong LY, Ling XY, Nduom E, et al. Effect of miR-142-3p on the M2 macrophage and therapeutic efficacy against murine glioblastoma. *J Natl Cancer Inst*. (2014) 106(8). doi: 10.1093/jnci/dju162

21. Yang J, Zhang Z, Chen C, Liu Y, Si Q, Chuang TH, et al. MicroRNA-19a-3p inhibits breast cancer progression and metastasis by inducing macrophage polarization through downregulated expression of Fra-1 proto-oncogene. *Oncogene*. (2014) 33(23). doi: 10.1038/onc.2013.258

22. Cai X, Yin Y, Li N, Zhu D, Zhang J, Zhang CY, et al. Re-polarization of tumor-associated macrophages to pro-inflammatory M1 macrophages by microRNA-155. *J Mol Cell Biol*. (2012) 4. doi: 10.1093/jmcb/mjs044

23. Graff JW, Dickson AM, Clay G, McCaffrey AP, Wilson ME. Identifying functional microRNAs in macrophages with polarized phenotypes. *J Biol Chem*. (2012) 287(26):21816–25. doi: 10.1074/jbc.M111.327031

24. Liu G, Abraham E. MicroRNAs in immune response and macrophage polarization. *Arterioscler Thromb Vasc Biol*. (2013) 33(2). doi: 10.1161/ATVBAHA.112.300068

25. Brun J, McManus D, Lefebvre C, Hu K, Falls T, Atkins H, et al. Identification of genetically modified maraba virus as an oncolytic rhabdovirus. *Mol Ther*. (2010) 18(8). doi: 10.1038/mt.2010.103

26. Ilkow CS, Marguerie M, Batenchuk C, Mayer J, Ben Neriah D, Cousineau S, et al. Reciprocal cellular cross-talk within the tumor microenvironment promotes oncolytic virus activity. *Nat Med*. (2015) 21(5). doi: 10.1038/nm.3848

10.3389/fimmu.2024.1500570

Glossary

CAF	Cancer-associated fibroblast
ELISA	Enzyme-linked immunosorbent assay
HGSOC	High-grade serous ovarian cancer
HR	Homologous recombination
ICB	Immune checkpoint blockade
miRNA	microRNA
NTA	Nanoparticle tracking analysis
NTC	Non-targeting control
ORV	Oncolytic Rhabdovirus
OVA	Ovalbumin
OvCa	Ovarian cancer
OVs	Oncolytic Viruses
PARPi	Poly-ADP ribose polymerase inhibitors
PBMC	Peripheral blood mononuclear cell
SSC	Side Scatter
TAM	Tumour-associated macrophage
TDEVs	Tumour derived extracellular vesicles
TME	Tumour microenvironment